THE BALTIC JOURNAL
OF ROAD AND BRIDGE ENGINEERING

ISSN 1822-427X / eISSN 1822-4288
2017 Volume 12(1): 12–20

IMPACT OF FIBER DIAMETER ON-ROAD PERFORMANCE OF CEMENT-STABILIZED MACADAM

Zhijun Liu[1]✉, Dongquan Wang[2], Xiaobi Wei[3], Liangliang Wang[4]

State Key Laboratory for Geomechanics and Deep Underground Engineering, School of Mechanics & Civil Engineering, China University of Mining & Technology, No. 1 University Road, Xuzhou 221116, China
E-mails: [1]liuzhijun0331@cumt.edu.cn; [2]wangdq@cumt.edu.cn; [3]weixb@cumt.edu.cn; [4]wallcn@cumt.edu.cn

Abstract. Cement-stabilized macadam is the most widely used road base material in road engineering. The current study investigated the impact of fiber diameter on its performance. The authors prepared polyester fibers with diameters of 20, 35, 70, and 105 μm and added them to cement-stabilized macadam. Then, the indoor shrinkage tests and mechanical property tests at different ages were conducted. Then, the property changes of the polyester-reinforced cement-stabilized macadam were analysed. The water loss rate of the polyester-reinforced cement-stabilized macadam is subject to the combined influence of the "water loss surface effect" and "water loss porthole effect." With increasing fiber diameter, the water loss surface effect becomes stronger, and the water loss porthole effect gradually decreases; thus, the overall effect transitions from the latter to the former. Moreover, the water loss rate shows an increasing trend of decreasing to its minimum. Therefore, with increasing fiber diameter, the average dry shrinkage coefficient of the polyester-reinforced cement-stabilized macadam first increases and then decreases, while the temperature shrinkage coefficients increase. The change in the fiber diameter does not significantly affect the compressive resilient modulus of the polyester-reinforced cement-stabilized macadam if the fiber content remains constant. These findings demonstrate the functional mechanism of the fiber diameter on the road performance of cement-stabilized macadam, thus improving our understanding of the road performance of the polyester-reinforced cement-stabilized macadam and laying a solid theoretical foundation for its many applications.

Keywords: experimental study, fiber diameter, polyester-reinforced cement-stabilized macadam (PETCSM), shrinkage crack, strength.

1. Introduction

Cement-stabilized macadam, which exhibits high strength, excellent crack resistance, and strong erosion resistance, is the most commonly used semi-rigid base material (Berthelot *et al.* 2010; Jitsangiam *et al.* 2016). However, the major disadvantage of cement-stabilized macadam is that it is prone to cracking (Ma *et al.* 2007a, 2007b, 2007c; Taha *et al.* 2002; Wang *et al.* 2010). This crackig is mainly a result of material dehydration and temperature changes, which cause dry shrinkage and temperature shrinkage, respectively (Norling 1973; Wang *et al.* 2008). The road base, which is the main bearing layer, sustains vehicle loads relayed from the upper parts of the road structure. Therefore, cracks in the cement-stabilized macadam base can easily lead to reflection cracks in asphalt pavement (Gibney *et al.* 2002; Nusit, Jitsangiam 2016; Scullion 2002), allowing rain to infiltrate into the base course, which decreases the overall road strength and greatly impacts the service life (Blankenship *et al.* 2004; Liu 2015b). Research on the prevention of cracks in cement-stabilized macadam has received significant attention over the past few years

For many years, scholars have conducted extensive work in this field and have proposed a variety of preventive measures (Grilli *et al.* 2013; Shahu *et al.* 2013; Siripun *et al.* 2011), including improving the mixture gradation method (Hu *et al.* 2001), improving the method of paving the cement-stabilized macadam base (Wang, Zhou 2006), and including certain additives, such as expansive agents and shrinkage reducing agents (e.g., waste asphalt concrete fibers), to improve the crack resistance (Farhan *et al.* 2015; Li *et al.* 2013; Li, Zheng 2009; Liao *et al.* 2012). Research has shown that adding fiber, one of the main types of additives, can improve the material's crack resistance to a certain extent and improve the compressive strength, splitting strength, and compressive resilient modulus (CRM) (Cavey *et al.* 1995; Wu *et al.* 2011). To date, research investigations have concentrated on polypropylene fiber, steel

doi:10.3846/bjrbe.2017.02

fiber, and glass fiber as additives (Kaniraj, Havanagi 2001; Khattak, Alrashidi 2006; Namdar *et al.* 2012; Zhang *et al.* 2013). However, the literature has only recently considered polyester as an additive for improving the crack resistance of cement-stabilized macadam.

Polyester fiber has relatively good chemical stability, acid resistance, microbial resistance, and strong anti-erosion ability. It boasts high strength, moderate extension, a high modulus, and good rebound resilience and has the best overall performance among the soft fibers (Sun 2006). Since the 1970s, extensive research has been conducted on the addition of polyester fibers to asphalt concrete surfaces to improve road performance (Moussa, Gomaa 2003; Ting *et al.* 2002), and scholars have achieved promising results. Liu *et al.* (2009) and Liu and Lv (2009) analysed and obtained the water loss rate and shrinkage coefficient of polyester-reinforced cement-stabilized macadam (PETCSM) via shrinkage tests and found that the road performance index varied with age, fiber content, and length. They concluded that the fiber length of PETCSM should be 5 mm and that the optimal content is 0.7‰. Zhao *et al.* (2014) and Liu (2015a) performed indoor mechanical tests to study the impacts of the length, content, and age of the polyester fiber on the unconfined compressive strength, splitting strength, and resilient modulus of cement-stabilized macadam. According to them, polyester fiber better improves the mechanical strength of cement-stabilized macadam than polypropylene fiber. Xu (2012) studied the impacts of the length and content of the polyester fiber on the flexural strength of cement-stabilized macadam via indoor tests.

In summary, adding polyester fibers for crack prevention and improvements in road performance has shown favourable results. However, there is still a lack of research on the impact of fiber diameter on the shrinkage and strength of cement-stabilized macadam. Therefore, this study examines the impact of fiber diameter on the shrinkage and strength of cement-stabilized macadam to extend the PETCSM research results and to establish a theoretical foundation for its many applications in road construction projects.

2. Materials and methods

2.1. Materials

The cement used in the experiment was Hanbang P·O32.5 ordinary Portland cement (Huaihai Cement Plant, Xuzhou, China). Table 1 shows its main technical characteristics. The aggregates, which were limestone, were all the products of the plant. Table 2 shows the grain gradation of the aggregates for an aggregate crushing value of 23.7%. The PET polyester fiber was made by Taian Modern Plastic Co. Ltd., China (Fig. 1a), with a circular cross-section and a length of 50 mm. Table 3 shows its main technical characteristics.

2.2. Mixing proportions

In the experiment, the cement content in the cement-stabilized macadam was 4.5%, which is a value commonly used in engineering, and the polyester fiber content was 0.5%, by the literature (Banthia, Gupta 2006). Four fiber diameters – 20 μm, 35 μm, 70 μm, and 105 μm – were considered to study the impact of fiber diameter on the road performance indexes of cement-stabilized macadam (Fig. 1b). The standard compaction test indicated that the

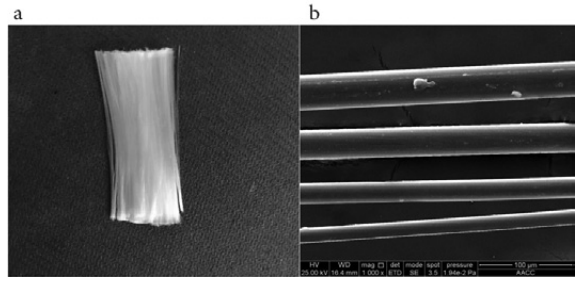

Fig. 1. Polyester fiber: a – unmagnified (single type); b – polyester fibers with diameters of 20, 35, 70, and 105 μm (magnified 1 000× under an electron microscope)

Table 1. Technical characteristics of the cement

Loss on ignition, %	Fineness sieving residue, % (80 μm square hole sieve)	Setting time		Compressive strength, MPa		Flexural strength, MPa	
		Initial setting time	Final setting time	3 days	28 days	3 days	28 days
<5	<10	≥45 min	≥6 h	≥16	≥32.5	≥3.5	≥6.5

Table 2. Aggregate gradation

Size of the square hole sieve, mm	31.5	26.5	19	9.5	4.75	2.36	0.6	0.075
Passing rate, %	100	95	80.5	57	39	21.5	11.5	1.8

Table 3. Technical characteristics of the polyester fiber

Type (code)	Proportion, $g \cdot cm^{-3}$	Melting point, °C	Thermal conductivity	Acid- and alkali-resistance	Ductility, %	Tensile strength, MPa	Elastic modulus, MPa	Coefficient of thermal expansion, 10^5 °C
PET	1.36	>250	low	strong	35	960	≥9 000	5–6

maximum dry density and optimum water content of the mixture were 2.33 g/ cm^3 and 5.50%, respectively.

2.3. Specimen preparation

According to the shrinkage test method for PETCSM in *JTG E51-2009 Test Methods of Materials Stabilized with Inorganic Binders for Highway Engineering*, the authors did not use cylindrical specimens for shrinkage tests (Liu 2015a) in this study but 100×100×400 mm beam specimens to obtain dry shrinkage coefficient and temperature shrinkage coefficient. The authors added polyester fibers with four different diameters to each specimen, with six parallel dry shrinkage specimens and three parallel temperature shrinkage specimens. The specimens used in the mechanical properties test used the more common cylindrical specimens with a diameter of 150 mm and a height of 150 mm; three properties were measured: the unconfined compressive strength, splitting strength, and CRM. 13 parallel specimens were molded using the static pressure method, and the authors controlled the degree of compactionat 98%.

2.4. Test methods

Experimental tests were performed according to the methods prescribed in *JTG E51-2009*.

(1) Dry shrinkage test.

After the specimens had been moulded using the static pressure method, they were placed into a thermostatic curing chamber for seven days before the test. First, the initial values of the specimen height and weight were measured. The authors placed three parallel specimens on a contractometer (Fig. 2). In the natural water loss and dry state, the authors measured the side specimens at the same time once per day. The masses of the other three parallel specimens were measured and their water loss rates were calculated and recorded; the readings on the dial gauge of the contractometer were registered at the same time every day. The authors took the readings on the micrometre until their average values did not change for three days; then, the dry shrinkage test was completed.

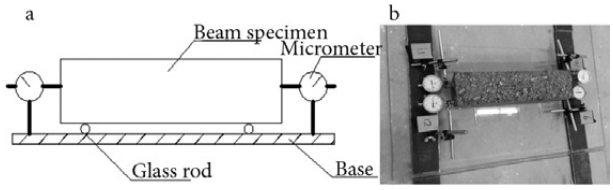

Fig. 2. Shrinkage test of the beam specimen: a – layout chart; b – test

Fig. 3. Shrinkage test

The parameters for the shrinkage performance were calculated according to Eqs (1)–(5).

$$w_i = \frac{m_i + m_{i+1}}{m_p}, \tag{1}$$

$$\delta_i = \frac{\sum_{j=1}^{4} X_{i,j} - \sum_{j=1}^{4} X_{i+1,j}}{2}, \tag{2}$$

$$\varepsilon_i = \frac{\delta_i}{l}, \tag{3}$$

$$\alpha_{di} = \frac{\varepsilon_i}{w_i}, \tag{4}$$

$$\alpha_d = \frac{\sum \varepsilon_i}{\sum w_i}, \tag{5}$$

where w_i – the water loss rate, %, at the i^{th} measurement; δ_i – the dry shrinkage observed at the i^{th} measurement, i.e., the readings from the two meters at each end of the beam were averaged, and the average values, mm, at both ends were added; ε_i – the dry shrinkage strain, %, at the i^{th} measurement; α_{di} – the dry shrinkage coefficient at the i^{th} measurement; α_d – the total dry shrinkage coefficient; m_i – the weighed mass of the standard specimen at the i^{th} measurement; m_{i+1} – the weight of the standard specimen, g, at the i+1th measurement; $X_{i,j}$ – the reading on the j^{th} dial gauge at the ith measurement; $X_{i+1,j}$ – the reading of the j^{th} dial gauge at the i+1th measurement, mm; l – the length, mm of the standard specimen; m_p – the mass, g, of the dried standard specimen.

(2) Temperature shrinkage test.

After moulding the specimens, they were cured in a thermostatic chamber for seven days. Then, they were dried to a constant weight in a high-temperature oven, and their heights were measured. The authors controlled the experimental temperature between 40 °C and 0 °C (Fig. 3). First, the specimens were placed in a constant-temperature environment of 40 °C in a high- and the low-temperature control chamber and the readings on the dial gauge after four hours were recorded. Then, the temperature was lowered to 0 °C, and the readings on the dial indicator after four hours were registered. Then, the authors finished the temperature shrinkage experiment.

The parameters for the temperature shrinkage performance were calculated according to Eqs (6) and (7):

$$\varepsilon = \frac{l_b - l_f}{L_0}, \tag{6}$$

$$\alpha_t = \frac{\varepsilon}{t_b - t_f}, \quad (7)$$

where ε – the average shrinkage strain, %, within the temperature variation range; l_b – the shrinkage at the initial thermostatic high temperature of 40 °C, i.e., the readings from the two meters at each end of the beam were averaged, and the average values (mm) at both ends were added; l_f – the shrinkage at the final thermostatic low temperature of 0 °C (mm); L_0 – the length, mm, corresponding to the constant weight of the dried specimen; α_t – the average dry shrinkage coefficient, %, in the temperature variation range; t_b – the initial stable high temperature, 40 °C; and t_f – the final shrinkage at the stable low temperature, 0°C.

(3) Mechanical performance test.

After moulding, the authors cured the specimens for the compressive strength and splitting strength tests for 7, 28, 60, or 90 days. Then, the specimens were cured for the CRM test for 60 or 90 days. The authors measured and calculated the compressive strength, splitting strength and CRM for the specimens at the ages prescribed by *JTG E51-2009* (Fig. 4).

The parameter values of the mechanical properties were calculated according to Eqs (8)–(10):

$$R_c = 0.00005659 \cdot P, \quad (8)$$

$$R_i = 0.004178 \cdot \frac{P}{h}, \quad (9)$$

$$E_c = \frac{p \cdot h}{l}, \quad (10)$$

where R_c – the unconfined compressive strength, MPa, of the specimen; R_i – the splitting strength, MPa, of the specimen; P – the maximum pressure, N, when the specimen failed; E_c – the CRM, MPa, of the specimen; p – the unit pressure, MPa; l – the rebound deformation, mm, of the specimen.

3. Results and discussion

3.1. Relation between the dry shrinkage coefficient and fiber diameter

Table 4 summarizes the statistical data related to the dry shrinkage experiments.

The authors averaged the dry shrinkage coefficients of the parallel PETCSM specimens, and the curve shows the relation between the dry shrinkage coefficient. Fig. 5 gives fiber diameter.

In Fig. 5, the average dry shrinkage coefficients of the PETCSM first decrease and then increase with increasing fiber diameter. The change in fiber diameter influences the shrinkage of the mix: the shrinkage coefficient is relatively large when the fiber diameter is small. Water loss is the main reason for the shrinkage of cement-stabilized macadam (Banthia, Gupta 2006), and two main factors influence the water loss rate. One factor is the "water loss surface effect": the addition of fiber effectively reduces the water loss surface on the material surface, hindering water migration; as a result, the capillary tension formed by capillary water loss shrinkage decreased (Yang 2003), decreasing the water loss rate. The other factor is the "water loss porthole effect": the basic composition of cement-stabilized macadam consists of grains, and the portholes, formed by fibers running through the specimen straight to the surface, increase the water loss rate. Figure 6 shows the

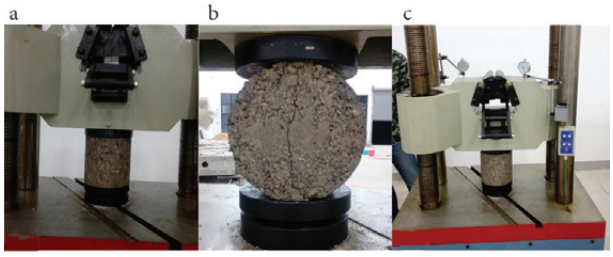

Fig. 4. Mechanical performance test: a – unconfined compressive strength test; b – splitting strength test; c – CRM test

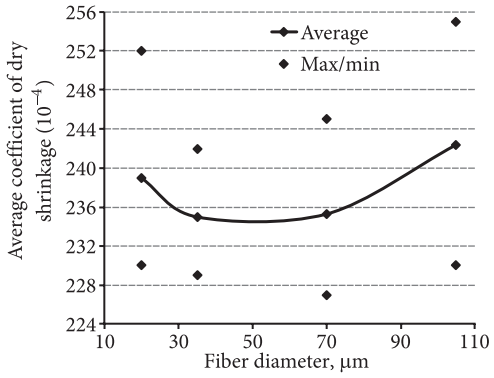

In this Fig. change to English UK Fiber diameter, μm

Fig. 5. Relation between the dry shrinkage coefficient and fiber diameter

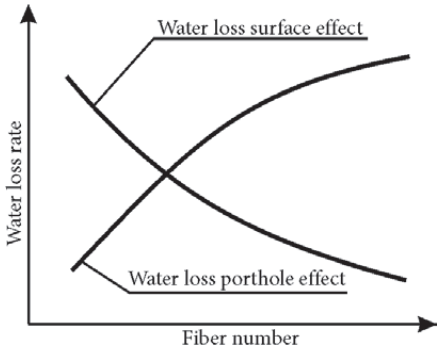

In this Fig. change to English UK Fiber diameter, μm

Fig. 6. Factors influencing the water loss rate

Table 4. Statistical data related to the dry shrinkage experiments

Fiber diameter, μm	Dry shrinkage coefficient (10^{-4})			Coefficient of variation, %
	Average	Maximum	Minimum	
20	239	252	230	4.83
35	235	242	229	2.79
70	235	245	227	3.86
105	243	255	230	5.16

relation between the fiber diameter and the water loss rate as influenced by these two factors.

For the same fiber mass and fiber length, larger diameter results in fewer filaments. A low number of filaments associates with high water loss on the surface of the specimen and an increase in the water loss rate. Decreasing the number of portholes decreases the water loss rate. As shown in Fig. 6, an excessively small fiber diameter and a larger number of filaments increase the magnitude of the water loss porthole effect, as indicated by the relatively large water loss rate and dry shrinkage coefficient for PETCSM. The porthole effect gradually decreases, and the water loss surface effect gradually increases with increasing fiber diameter decreasing filament number because of the water loss rate and dry shrinkage coefficient decrease. However, further increases in the fiber diameter result in further decreases in the filament number. Thus, the water loss effect becomes more significant than the porthole effect at larger fiber diameters. As a result, the water loss rate of the specimen increases, and the dry shrinkage coefficient increases again.

3.2. Relation between the temperature shrinkage coefficient and fiber diameter

Table 5 summarizes the statistical data related to the temperature shrinkage experiments.

The authors averaged the shrinkage coefficients of the parallel PETCSM specimens, and Fig. 7 shows the relation between the temperature shrinkage coefficient and fiber diameter.

Table 5. Statistical data related to the temperature shrinkage experiments

Fiber diameter, μm	Temperature shrinkage coefficient, 10^{-6}/°C			Coefficient of variation, %
	Average	Maximum	Minimum	
20	5.11	5.29	5.01	3.06
35	5.20	5.47	5.01	4.62
70	5.50	5.76	5.21	4.24
105	5.90	6.38	5.60	7.12

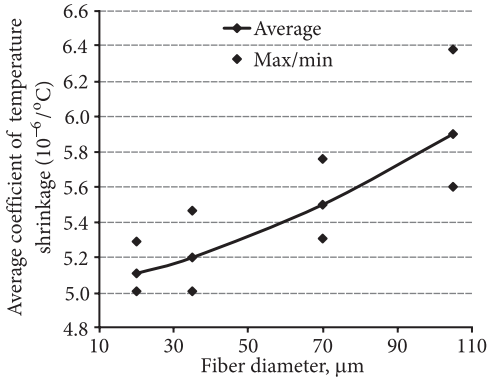

In this Fig. change to English UK Fiber diameter, μm

Fig. 7. Relation between the temperature shrinkage coefficient and fiber diameter

Figure 7 shows that the average temperature coefficient of PETCSM increases with the fiber diameter. The polyester added to the cement-stabilized macadam mix takes on a random three-dimensional distribution. With increasing age, the fiber and cement-stabilized macadam base further cement into a solid whole. Changes in the outside temperature cause the base to contract or expand. Compared with cement-stabilized macadam, the thermal expansion coefficient of the polyester fibers is small, thus inhibiting the base's contraction or expansion (Yang 2003). When added polyester is in the same mass and with the same length, a smaller fiber diameter associates with a higher filament number. Here, the temperature shrinkage coefficient is rather small, indicating that the added fiber strongly inhibits the deformation of the base caused by a temperature change. This trend occurs because the three-dimensional distribution of the additional filaments in the base is rather compact, effectively inhibiting base deformation. In contrast, when the fiber diameter increases, the filament number decreases; thus, the filaments within the base become sparser, leading to a weaker inhibition effect for base deformation. The results show the trend that the temperature coefficient increases with the fiber diameter.

3.3. Relation between the strength and fiber diameter

Table 6 presents the statistical data for the strength experiments.

Figure 8 presents the curve showing the relation between the PETCSM strength and fiber diameter.

Figure 8 shows that at the same age and the same fiber content, both the compressive strength and splitting strength of PETCSM decrease linearly with increasing fiber diameter. However, a shorter age leads to a narrower range of decrease. At the age of 7 days, the compressive strength and splitting strength of PETCSM with a fiber diameter of 105 μm are 6.8% and 14.3% lower, respectively, than those of PETCSM with a fiber diameter of 20 μm. Furthermore, older age associates with a more rapid decline. At the age of 90 days, the compressive strength and splitting strength of PETCSM with a fiber diameter of 105 μm are 23.6% and 38.9% lower, respectively, than those of PETCSM with a fiber diameter of 20 μm. This trend occurs because the cement-stabilized macadam mixes bonds with the added fiber through physical and chemical reactions. When bonded to each other, the fiber and the bonding base display a high tensile strength through friction and the pulling effect, thus increasing the strength of the bonding base (Yang 2003). When the base finally breaks under the action of an external force, which pulls out the fiber from the base (but the fiber does not typically break) (Fig. 9). In other words, the fiber displays high tensile strength through the pulling effect caused by the frictional contact between the fiber surface and base. Therefore, two main factors influence the final strength of PETCSM: the size of the contact area between the fiber and base and the solid degree of the contact area between the fiber and the base. Eq (11) shows the basic relationship between the contact area of the fiber and cemented body and the fiber diameter.

Table 6. Statistics for the strength experiments

Age, days	Fiber diameter, μm	Unconfined compressive strength, MPa			CV, %	Splitting strength, MPa			CV, %
		Average	Maximum	Minimum		Average	Maximum	Minimum	
7	20	3.80	4.21	3.45	5.83	0.28	0.33	0.26	6.84
	35	3.75	4.23	3.11	8.54	0.28	0.32	0.26	5.26
	70	3.65	4.08	3.12	7.57	0.26	0.3	0.24	6.08
	105	3.54	4.19	3.01	7.70	0.24	0.28	0.21	7.61
28	20	5.30	5.74	4.65	6.56	0.43	0.49	0.39	6.23
	35	5.10	5.57	4.74	4.45	0.4	0.45	0.32	7.36
	70	4.80	5.54	4.32	6.91	0.35	0.38	0.32	4.81
	105	4.50	4.89	4.06	5.14	0.30	0.35	0.27	7.33
60	20	6.30	6.92	5.78	6.59	0.65	0.70	0.60	4.02
	35	6.10	6.75	5.64	5.46	0.60	0.63	0.56	3.33
	70	5.60	6.33	5.21	5.90	0.52	0.57	0.48	4.37
	105	5.10	5.65	4.75	4.66	0.42	0.45	0.39	4.45
90	20	7.20	7.55	6.91	3.36	0.77	0.85	0.70	4.31
	35	6.85	7.51	6.18	5.17	0.72	0.75	0.68	3.26
	70	6.15	6.71	5.72	4.39	0.60	0.68	0.56	5.05
	105	5.50	6.12	5.19	4.38	0.47	0.53	0.40	7.22

CV – coefficient of variation.

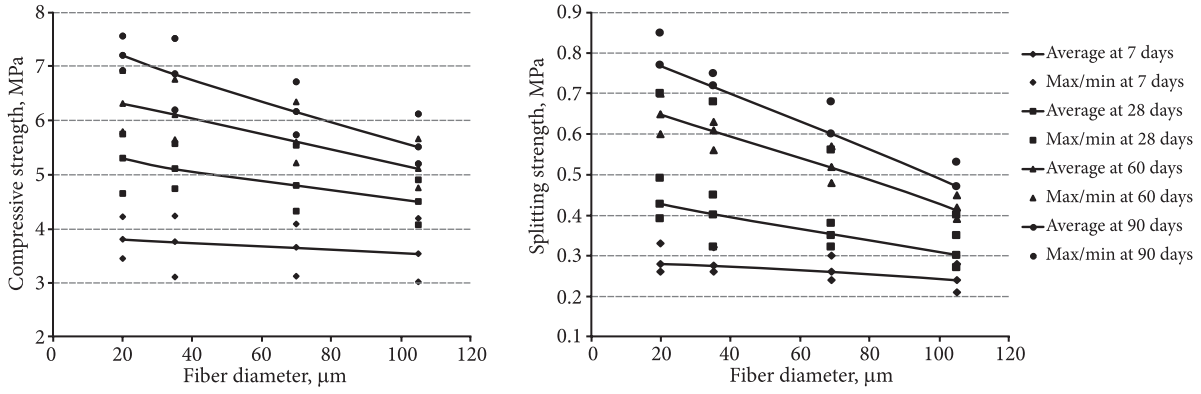

In this Fig. change to English UK Fiber diameter, μm

Fig. 8. Relation between PETCSM strength and fiber diameter: a – compressive strength; b – splitting strength

$$A = 4\frac{m}{D \cdot \rho}, \quad (11)$$

where A – the contact area, mm^2, between the fiber and base; m – the mass of the fiber; D – the fiber diameter, mm; ρ – the fiber density (g/mm^3). Eq (11) shows that at the same mass, the contact area between the fiber and base is inversely proportional to the fiber diameter, i.e., the contact area decreases linearly with increasing fiber diameter. The friction between the fiber and base and the pulling effect clearly decrease with decreasing strength. Xu (2012) compared the effects of fibers with different shapes and found that the bonded area between the fiber and cement-stabilized macadam base affects the friction and pulling effect. Regarding the solidness of the bond between the fiber and base contact area, at a younger age, the hydration reaction in the material has just started, and the generated cement

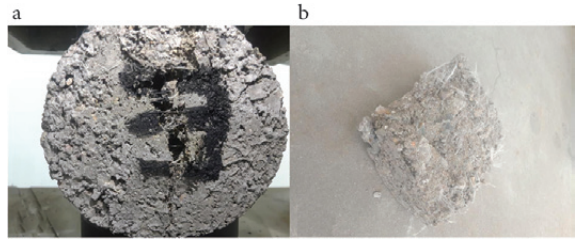

Fig. 9. Fiber status when the cement-stabilized macadam fails: a – crack gap; b – fracture surface

is only in a small amount. Early on, the mix is still in a relatively unstructured state that is inadequate for bonding the fiber and cement-stabilized macadam into a solid whole. Therefore, the solidness of the bond is relatively low, with weak anti-friction and anti-pulling effects. Here, diameter does not influence the strength significantly. A greater age

results in a more mature cementing body, and a more solid bond between the fiber and base results in stronger anti-friction and anti-pulling effects. The diameter significantly influences the strength, and the rate of decline increases with increasing fiber diameter.

In summary, the combined factors of the size of the contact area between the fiber and base and the solidness of the bond influence the strength of PETCSM. A larger contact area and more solid bond result in a higher strength, more specifically, a smaller diameter and older age lead to a higher strength. The evenness of the three-dimensional distribution of the fiber is also worth considering. For the same mass, a smaller diameter means more fiber filaments, which makes it easier for clustering to occur. This condition leads to low evenness, which in turn influences the PETCSM strength improvement. Therefore, the fiber diameter should not be excessively small in practical applications.

3.4. Compressive resilient modulus

Table 7 summarizes the statistical data for the CRM experiments.

Figure 10 shows the relation between the CRM and fiber diameter.

In Fig. 10, the CRM of PETCSM at the two different ages do not exhibit significant changes with increasing fiber diameter, i.e., at the same mass, a change in the fiber diameter does not significantly influence the CRM of the mix. This phenomenon also corroborates the analysis performed in studies on the impact of fiber content on the CRM (Liu, 2015a, 2015b; Yang 2003). The elastic modulus of the fiber is extremely high, compared to the mature plastic cementing body of cement-stabilized macadam. Therefore, the addition of fiber changes the ratio of the elastic and plastic properties to a certain degree. With increasing fiber content, the mix shifts from being "plastically" strong to being "elastically" strong. The proportion of the fiber content to the base mainly determines the CRM of cement-stabilized macadam reinforced with fiber. For the same fiber content, the ratio of the elastic and plastic properties of the base reinforced with fiber does not change regardless of the fiber diameter. Therefore, the CRM does not significantly change with variations in the fiber diameter.

Table 7. Statistical data for the CRM experiments

Age, days	Fiber diameter, μm	Compressive resilient modulus, MPa			Coefficient of variation, %
		Average	Maximum	Minimum	
60	20	1.32	1.42	1.19	4.25
	35	1.33	1.45	1.18	5.53
	70	1.31	1.41	1.20	3.87
	105	1.32	1.42	1.27	3.29
90	20	1.45	1.54	1.31	4.52
	35	1.46	1.52	1.31	3.96
	70	1.43	1.51	1.35	3.05
	105	1.45	1.54	1.36	3.40

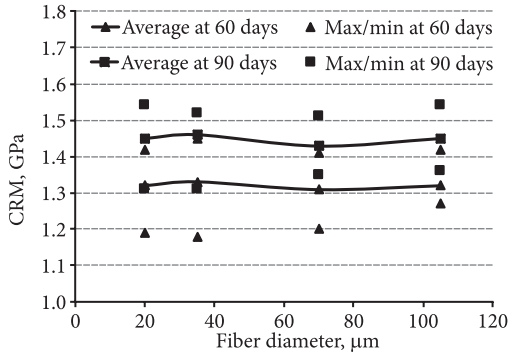

Fig. 10. The relation between the CRM of PETCSM and fiber diameter

4. Conclusions

This study conducted indoor physical tests on polyester-reinforced cement-stabilized macadam with different fiber diameters and found that changes in the polyester fiber diameter influenced the shrinkage and strength. We also analysed the working mechanism to provide additional information about the impact of polyester fibers on the road performance of cement-stabilized macadam.

1. The fiber diameter influences the dry shrinkage performance of the polyester-reinforced cement-stabilized macadam mix. With increasing fiber diameter, the average dry shrinkage coefficients of polyester-reinforced cement-stabilized macadam first decreased and then increased.

2. The "water loss surface effect" and "water loss porthole effect" influence the water loss rate of polyester-reinforced cement-stabilized macadam. With increasing fiber diameter, the effect of water-loss surface becomes stronger, whereas the porthole effect gradually decreases at the same fiber content. The effect transitioned from the water loss porthole effect to the water loss surface effect, and the water loss rate increased after decreasing to a minimum.

3. When adding polyester fiber of the same mass and same length into cement-stabilized macadam, the fiber filament number increases with decreasing fiber diameter. As a result, the fiber was more efficient for inhibiting the deformation of the base caused by a temperature change. Conversely, when the fiber diameter increased, the filament number decreased; as a result, the filaments within the base became more spread out, leading to a less efficient inhibition of the deformation of the cement-stabilized macadam base. As a result, the temperature shrinkage coefficient increased with the fiber diameter.

4. At the same fiber content and age, both the compressive strength and splitting strength of polyester-reinforced cement-stabilized macadam linearly decreased with increasing fiber diameter. Younger age was associated with a smaller range of decline, whereas the decline was more rapid at older ages.

5. The polyester-reinforced cement-stabilized macadam strength was subject to the combined influence of the contact area between the fiber and base and the solidness

of the bond. The fiber diameter was inversely proportional to the contact area, i.e., a smaller diameter and older age led to a higher strength.

6. After the addition of fiber to the cement-stabilized macadam, the fiber content in the base became the primary influencing factor for the material's compressive resilient modulus. At the same fiber content, the ratio of the elastic and plastic properties of the base materials reinforced by fiber remained unchanged regardless of the fiber diameter. The compressive resilient modulus of polyester-reinforced cement-stabilized macadam did not significantly change with varying fiber diameter.

In practical applications of polyester-reinforced cement-stabilized macadam, the fiber diameter should be determined based on the full consideration of shrinkage performance and strength. Although the fiber diameter can be obtained based on the dry shrinkage experiment (i.e., the diameter when the dry shrinkage coefficient reaches the minimum), we should decrease the diameterappropriately when there is a high strength requirement for the polyester-reinforced cement-stabilized macadam.

Acknowledgements

This study was supported by the Excellent State Key Laboratory Foundation (Grant No. 51323004) and the Transportation Research Project of Jiangsu Province *The Crack Resistance and Engineering Application of the Polyester Fiber-Reinforced Cement-Stabilized Macadam Base* (Grant No. 2014Y02G).

References

Banthia, N.; Gupta, R. 2006. Influence of Polypropylene Fiber Geometry on Plastic Shrinkage Cracking in Concrete, *Cement and Concrete Research* 36: 1263–1267. https://doi.org/10.1016/j.cemconres.2006.01.010

Berthelot, C.; Podborochynski, D.; Marjerison, B.; Saarenketo, T. 2010. Mechanistic Characterization of Cement Stabilized Marginal Granular Base Materials for Road Construction, *Canadian Journal of Civil Engineering* 37: 1613–1620. https://doi.org/10.1139/L10-102

Blankenship, P.; Lker, N.; Drbohlav, J. 2004. Interlayer and Design Considerations to Retard Reflective Cracking, *Transportation Research Record* 1896: 177–186. https://doi.org/10.3141/1896-18

Cavey, J. K.; Krizek, R. J.; Sobhan, K.; Baker, W. H. 1995. Waste Fibers in Cement-Stabilized Recycled Aggregate Base Course Material, *Transportation Research Record* 1486: 97–106.

Farhan, A. H.; Dawson, A. R.; Thom, N. H.; Adam, S.; Smith, M. J. 2015. Flexural Characteristics of Rubberized Cement-Stabilized Crushed Aggregate for Pavement Structure, *Materials & Design* 88: 897–905. https://doi.org/10.1016/j.matdes.2015.09.071

Gibney, A.; Lohan, G.; Moore, V. 2002. Laboratory Study of Resistance of Bituminous Overlays to Reflective Cracking, *Transportation Research Record* 1809: 184–190. https://doi.org/10.3141/1809-20

Grilli, A.; Bocci, M.; Tarantino, A. M. 2013. Experimental Investigation on Fibre-Reinforced Cement-Treated Materials Using Reclaimed Asphalt, *Construction and Building Materials* 38: 491–496. https://doi.org/10.1016/j.conbuildmat.2012.08.040

Hu, L. Q.; Jiang, Y. J.; Chen, Z. D.; Dai, J. L. 2001. Road Performance of Cement Stabilized Aggregate of Dense Framework Structure, *Journal of Traffic and Transportation Engineering* 4: 37–40 (in Chinese).

Jiang, Y. J.; Xue, H.; Xue, H.; Chen, Z. D. 2006. Preventing Cracks of Asphalt Pavement Based on Pre-Cutting Crack and Paving Geotextile at Semi-Rigid Type Base, *Journal of Chang'an University* (Natural Science Edition) 26: 6–9.

Jitsangiam, P.; Nusit, K.; Chummuneerat, S.; Chindaprasirt, P.; Pichayapan, P. 2016. Fatigue Assessment of Cement-Treated Base for Roads: an Examination of Beam-Fatigue Tests, *Journal of Materials in Civil Engineering* 28: 04016095. https://doi.org/10.1061/(ASCE)MT.1943-5533.0001601

Kaniraj, S. R.; Havanagi, V. G. 2001. Behavior of Cement-Stabilized Fiber-Reinforced Fly Ash-Soil Mixtures, *Journal of Geotechnical & Geoenvironmental Engineering* 127: 574–584. https://doi.org/10.1061/(ASCE)1090-0241(2001)127:7(574)

Khattak, J.; Alrashidi, M. 2006. Durability and Mechanistic Characteristics of Fiber Reinforced Soil-Cement Mixtures, *International Journal of Pavement Engineering* 7(1): 53–62. https://doi.org/10.1080/10298430500489207

Li, H. B.; Liu, Z. J.; Shen, H. 2013. Experimental Study on the Crack Resistance of Waste Asphalt Concrete Fiber Cement Stabilized Macadam, *Applied Mechanics & Materials* 405–408: 1786–1790. https://doi.org/10.4028/www.scientific.net/AMM.405-408.1786

Li, H. Z.; Zheng, J. L. 2009. Research on Shrinkage Performance of Cement-Stabilized Macadam Base Adding Reclaimed Asphalt Mixture, *International Conference on Energy and Environment Technology* 1: 292–296. https://doi.org/10.1109/ICEET.2009.76

Liao, X. F.; Xiao, F.; Zhong, D. C.; Xing, L. 2012. The Influence of Different Subbase Materials on the Crack of Cement Stabilized Macadam Base during Construction, *Advanced Materials Research* 591–593: 955–959. https://doi.org/10.4028/www.scientific.net/AMR.591-593.955

Liu, Z. J. 2015a. Experimental Research on the Engineering Characteristics of Polyester Fiber-Reinforced Cement-Stabilized Macadam, *Journal of Materials in Civil Engineering* 27(10): 04015004. https://doi.org/10.1061/(ASCE)MT.1943-5533.0001251

Liu, Z. J. 2015b. Influence of Rainfall Characteristics on the Infiltration Moisture Feld of High-Way Subgrade, *Road Materials and Pavement Design* 16(3): 635–652. https://doi.org/10.1080/14680629.2015.1021370

Liu, Z. J.; Bian, Z. F.; Liu, C. R.; Zhou, X. L.; Dai, S. C.; Ren, J. L. 2009. Experimental Study of Influence of Polyester Fibre on Shrinkage Cracks of Cement-Stabilized Macadam, *Journal of China University of Mining & Technology* 38: 155–158.

Liu, Z. J.; Lv, C. 2009. Experimental Study on Influence of Polyester Fibre on Anti-Cracking Performance of Cement-Stabilized Macadam, *Architecture Technology* 40: 449–451 (in Chinese).

Ma, B. G.; Wen, X. D.; Wang, M. Y.; Yan, J. J.; Guo, X. J. 2007a. Drying Shrinkage of Cement-Based Materials under Conditions of Constant Temperature and Varying Humidity, *Journal of China University of Mining and Technology* 17(3): 428–431. https://doi.org/10.1016/S1006-1266(07)60119-9

Ma, Y. H.; Yi, Z. J.; Yang, Q. G. 2007b. Analysis of Anti-Cracking and Tenacity Increasing Mechanism of Flexible Fiber Cement-Stabilized Material Semi-Rigid Base, *Journal of Chongqing Jiaotong University* 26(5): 84–86.

Ma, Y. H.; Zhang, G.; Yi, Z. J.; Zhong, Y. S.; Han, B. X. 2007c. Experimental Research on Flexural Toughness of Semi-Rigid Base Mixed into Polypropylene Fiber, *Journal of Chongqing Jiaotong University* 26(4): 57–60.

Moussa, J.; Gomaa, K. 2003. Effect of Addition of Short Fibers of Poly-Acrylic and Polyamide to Asphalt Mixtures, *AEJ Alexandria Engineering Journal* 42: 329–336.

Namdar, P.; Estabragh, A. R.; Javadi, A. A. 2012. Behavior of Cement-Stabilized Clay Reinforced with Nylon Fiber, *Geosynthetics International* 19(1): 85–92. https://doi.org/10.1680/gein.2012.19.1.85

Norling, L. T. 1973. Minimizing Reflective Cracks in Soil-Cement Pavement: A Status Report of Laboratory Studies and Field Practices, *Highway Research Record* 442: 22–33.

Nusit, K.; Jitsangiam, P. 2016. Damage Behavior of Cement-Treated Base Material, *Procedia Engineering* 143: 161–169. https://doi.org/10.1016/j.proeng.2016.06.021

Scullion, T. 2002. Precracking of Soil-Cement Bases to Reduce Reflection Cracking: Field Investigation, *Transportation Research Record* 1787: 22–30. https://doi.org/10.3141/1787-03

Shahu, J. T.; Patel, S.; Senapati, A. 2013. Engineering Properties of Copper Slag–Fly Ash–Dolime Mix and Its Utilization in the Base Course of Flexible Pavements, *Journal of Materials in Civil Engineering* 25(12): 1871–1879. https://doi.org/10.1061/(ASCE)MT.1943-5533.0000756

Siripun, K.; Jitsangiam, P.; Nikraz, H. 2011. The Use of Fibre Reinforced Crushed Rocks for the Improvement of Tensile Strength, in *Geo-Frontiers Congress*, 13–16 March 2011, Dallas, Texas, United States. 4449–4457. https://doi.org/10.1061/41165(397)455

Sun, L. L. 2006. *Experimental Study on Dynamic Modulus of Asphalt Concrete Reinforced by Polyester Fiber*: Dissertation, Dalian Maritime University, Dalian, China.

Taha, R.; Alharthy, A.; Alshamsi, K.; Alzubeidi, M. 2002. Cement Stabilization of Reclaimed Asphalt Pavement Aggregate for Road Bases and Subbases, *Journal of Materials in Civil Engineering* 14(3): 239–245. https://doi.org/10.1061/(ASCE)0899-1561(2002)14:3(239)

Ting, J. S.; Santoni, R. L.; Webster, S. L. 2002. Full Scale Field Tests of Discrete Fiber Reinforced Sands, *Journal of Transportation Engineering* 128(1): 9–16. https://doi.org/10.1061/(ASCE)0733-947X(2002)128:1(9)

Wang, Y.; Ni, F. J.; Li, Q.; Li, Z. X. 2008. Study on Controlling of Transverse Shrinkage Cracking in Cement Stabilized Macadam Base, *Journal of Highway and Transportation Research and Development* 25: 45–49.

Wang, Y.; Ma, X.; Sun, Z. L. 2010. Shrinkage Performance of Cement-Treated Macadam Base Materials, *Traffic and Transportation Studies* 13: 1386–1378. https://doi.org/10.1061/41123(383)132

Wang, Y. L.; Zhou, Y. L. 2006. Anti-Flexural-Tensile Strength Test of Semi-Rigid Type Base Course Materials Reinforced by Geogrid, *Journal of Chang'an University* (Natural Science Edition) 26: 26–29 (in Chinese).

Wu, W.; Zhang, C.; Wei, S. Z. 2011. Experimental Study on the Mechanical Performance of Cement-Stabilized Macadam Reinforced with Fiber, *International Conference on Transportation, Mechanical, and Electrical Engineering* 16–18: 1989–1991.

Yang, H. H. 2003. *Study on Anti-Crack of Cement with Expansion Agent or Fiber*: Dissertation, Chang'an University, Xi'an, China.

Xu, X. X. 2012. Experimental Research on the Flexural Performance of Cement-Stabilized Macadam Affected by Polyester Fiber-Reinforced, *Journal of China & Foreign Highway* 32: 297–300.

Zhang, P.; Liu, C. H.; Li, Q. F.; Zhang, T. H. 2013. Effect of Polypropylene Fiber on Fracture Properties of Cement Treated Crushed Rock, *Composites Part B Engineering* 55: 48–54 (in Chinese). https://doi.org/10.1016/j.compositesb.2013.06.005

Zhao, W. J.; Xue, J. S.; Yu, Y. Z. 2014. Effect of Polyester Fiber-Reinforced on the Rebound Modulus of Cement-Stabilized Macadam, *Journal of Highway and Transportation Research and Development* 2014: 89–91.

Received 9 August 2016; accepted 5 December 2016